



## Development of novel $\beta$ -amyloid probes based on 3,5-diphenyl-1,2,4-oxadiazole

Masahiro Ono<sup>a,b,\*</sup>, Mamoru Haratake<sup>a</sup>, Hideo Saji<sup>b</sup>, Morio Nakayama<sup>a</sup>

<sup>a</sup> Graduate School of Biomedical Sciences, Nagasaki University, 1-14 Bunkyo-machi, Nagasaki 852-8521, Japan

<sup>b</sup> Graduate School of Pharmaceutical Sciences, Kyoto University, 46-29 Yoshida Simoadachi-cho, Sakyo-ku, Kyoto 606-8501, Japan

### ARTICLE INFO

#### Article history:

Received 1 May 2008

Revised 23 May 2008

Accepted 24 May 2008

Available online 29 May 2008

#### Keywords:

Alzheimer's disease

$\beta$ -Amyloid

PET

SPECT

### ABSTRACT

In the search for novel probes for the imaging in vivo of  $\beta$ -amyloid plaques in Alzheimer's disease (AD) brain, we have synthesized and evaluated a series of 3,5-diphenyl-1,2,4-oxadiazole (DPOD) derivatives. The affinity for  $\beta$ -amyloid plaques was assessed by an in vitro-binding assay using pre-formed synthetic A $\beta$ 42 aggregates. The new series of DPOD derivatives showed excellent affinity for A $\beta$  aggregates with  $K_d$  values ranging from 4 to 47 nM. In biodistribution experiments using normal mice, [<sup>125</sup>I]**12**, [<sup>125</sup>I]**13**, [<sup>125</sup>I]**14**, and [<sup>125</sup>I]**15** examined displayed sufficient uptake for imaging, ranging from 2.2 to 3.3% ID/g. But the washout of the four ligands from the brain was relatively slow. Although additional modifications are necessary to improve the uptake and rapid clearance of non-specifically bound radiotracers, the DPOD pharmacophore with high-binding affinity for A $\beta$  aggregates may be useful as a backbone structure to develop novel  $\beta$ -amyloid imaging agents.

© 2008 Elsevier Ltd. All rights reserved.

### 1. Introduction

Alzheimer's disease (AD) is the most common neurodegenerative disorder of the elderly and is characterized clinically by dementia, cognitive impairment, and memory loss. The neuropathological hallmarks of AD include abundant deposits of  $\beta$ -amyloid plaques and neurofibrillary tangles. The deposition of  $\beta$ -amyloid plaques has been regarded as an initial event in the pathogenesis of AD.<sup>1,2</sup> Therefore, the quantitative evaluation of  $\beta$ -amyloid plaques in the brain with non-invasive techniques such as positron emission tomography (PET) and single photon emission computed tomography (SPECT) could lead to the presymptomatic detection of AD and new anti-amyloid therapies.<sup>3–5</sup>

Developing  $\beta$ -amyloid imaging probes is currently an emerging field of research. The basic requirements for suitable probes include (i) good penetration of the blood–brain barrier, (ii) selectively binding or labeling  $\beta$ -amyloid plaques, and (iii) displaying clear and contrasting signals between plaques and non-plaques. Based on these requirements, several promising agents with the backbone structure of DDNP, thioflavin-T, and Congo Red have been synthesized and evaluated for use in vivo as probes to image  $\beta$ -amyloid plaques in AD brain. Clinical trials in AD patients have been conducted with several agents including [<sup>18</sup>F]FDDNP,<sup>6,7</sup> [<sup>11</sup>C]6-OH-BTA-1,<sup>8,9</sup> [<sup>11</sup>C]SB-13,<sup>10,11</sup> [<sup>18</sup>F]BAY94-9172,<sup>12</sup> and [<sup>123</sup>I]IMPY<sup>13,14</sup> (Fig. 1) indicating the imaging of  $\beta$ -amyloid plaques in the living human brain to be useful for the diagnosis of AD.

Recently, a number of groups have reported new  $\beta$ -amyloid-binding probes without the basic structures of DDNP, thioflavin-T and Congo Red. Most of these probes have two aromatic rings. Among them, 1,4-diphenyltriazole and 2,5-diphenylthiophene derivatives have triazole and thiophene between two benzene rings, respectively, and it has been shown that they have tolerance for binding to A $\beta$  aggregates.<sup>15,16</sup> In an attempt to further develop novel ligands for the imaging of amyloid plaques in AD, we designed a series of 3,5-diphenyl-1,2,4-oxadiazole (DPOO) derivatives, in which triazole or thiophene of the 1,4-diphenyltriazole and 2,5-diphenylthiophene backbone was replaced with 1,2,4-oxadiazole. To our knowledge, this is the first time the use of DPOD derivatives in vivo as probes to image  $\beta$ -amyloid plaques in the AD brain has been proposed. Described herein is the synthesis of a novel series of DPOD derivatives and the characterization as  $\beta$ -amyloid imaging agents.

### 2. Results and discussion

The synthesis of the DPOD derivatives is outlined in Schemes 1 and 2. A wide variety of reaction conditions have been published for the synthesis of 3,5-diphenyl-1,2,4-oxadiazoles.<sup>17</sup> Among them, we used the reaction of an amidoxime with a carboxylic acid to form 1,2,4-oxadiazoles. In this process, the 3,5-diphenyl-1,2,4-oxadiazoles (**1** and **5**) were prepared by the condensation of 4-bromobenzamidoxime with 4-nitrobenzoic acid and 4-methoxybenzoic acid in the presence of DCC and HOBT. The amino derivative **2** was readily prepared from **1** by reduction with SnCl<sub>2</sub> (80.8% yield). Conversion of **2** to the monomethylamino derivative **3** was achieved by a method reported previously<sup>18</sup> (50.3% yield).

\* Corresponding author. Tel.: +81 75 753 4608; fax: +81 75 753 4568.  
E-mail address: [ono@pharm.kyoto-u.ac.jp](mailto:ono@pharm.kyoto-u.ac.jp) (M. Ono).

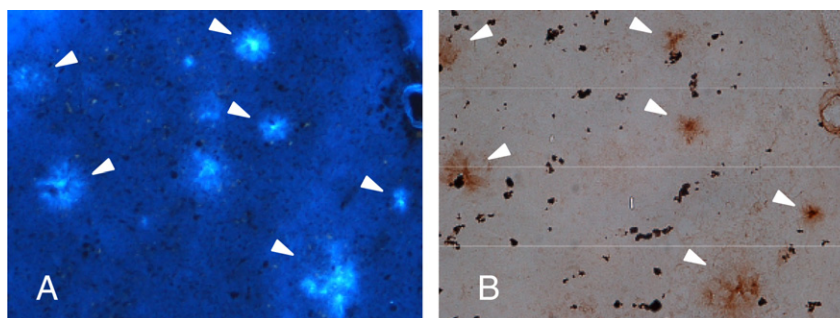
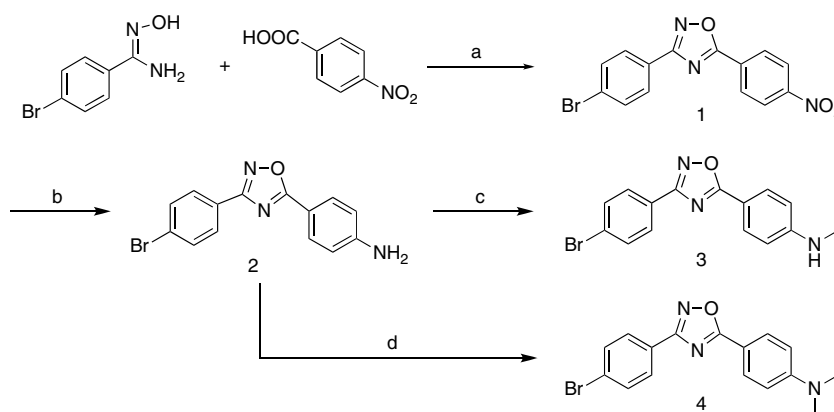
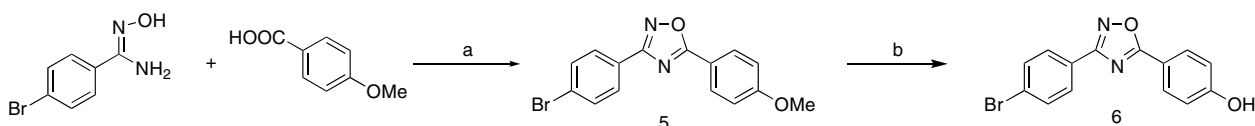


**Figure 1.** Neuropathological staining of compound **14** on 10- $\mu$ m AD model mouse sections. (A) Many  $\beta$ -amyloid plaques were clearly stained with **14**. (B) The serial sections were immunostained using an antibody against  $\beta$ -amyloid.



**Scheme 1.** (a) DCC, HOBT, DMF; (b) SnCl<sub>2</sub>, EtOH; (c) NaOMe, (CH<sub>2</sub>O)<sub>n</sub>, NaBH<sub>4</sub>, MeOH; (d) (CH<sub>2</sub>O)<sub>n</sub>, NaCNBH<sub>3</sub>, AcOH.



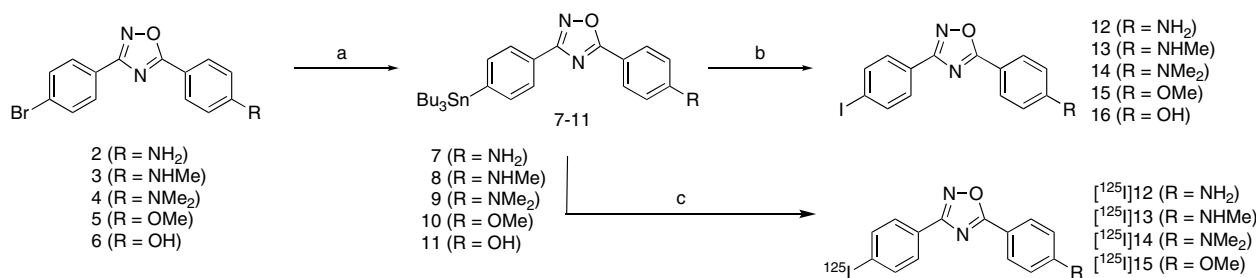
**Scheme 2.** (a) DCC, HOBT, DMF; (b) BBr<sub>3</sub>, CH<sub>2</sub>Cl<sub>2</sub>.

Compound **2** was also converted to the dimethylamino derivative **4** by an efficient method<sup>19</sup> with paraformaldehyde and acetic acid (68.4% yield). Compound **5** was converted to **6** by demethylation with BBr<sub>3</sub> in CH<sub>2</sub>Cl<sub>2</sub> (50.6% yield). The tributyltin derivatives (**7**, **8**, **9**, **10**, and **11**) were prepared from the corresponding bromo compounds (**2**, **3**, **4**, **5**, and **6**) using a bromo to tributyltin exchange reaction catalyzed by Pd(0) for yields of 16.8%, 15.8%, 20.3%, 22.8%, and 60.1%, respectively. These tributyltin derivatives were readily reacted with iodine in chloroform at room temperature to give the iodo derivatives (**12**, **13**, **14**, **15**, and **16**) for yields of 66.1%, 86.0%, 72.4%, 69.2%, and 81.8%. Furthermore, these tributyltin derivatives can be also used as the starting materials for radioiodination in the preparation of [<sup>125</sup>I]**12**, [<sup>125</sup>I]**13**, [<sup>125</sup>I]**14**, and [<sup>125</sup>I]**15**. Novel radioiodinated DPOD derivatives were achieved by an iododestannylation reaction using hydrogen peroxide as the oxidant which produced the desired radioiodinated ligands (Scheme 3). It was anticipated that the no-carrier-added preparation would result in a final product bearing a theoretical specific activity similar to that of <sup>125</sup>I (2200 Ci/mmol). The radiochemical identities of the radioiodinated ligands were verified by co-injection with non-radioactive compounds from their HPLC profiles. The final radioiodinated compounds, [<sup>125</sup>I]**12**, [<sup>125</sup>I]**13**, [<sup>125</sup>I]**14**, and [<sup>125</sup>I]**15**, showed a single peak of radioactivity at a retention time of 8.4, 15.7, 25.5, 22.3, and 7.1 min, respectively. Four radio-

iodinated products were obtained in 50–70% radiochemical yields with a radiochemical purity of >95% after HPLC.

The affinity of DPOD derivatives (compounds **12**, **13**, **14**, **15**, and **16**) was evaluated based on inhibition of the binding of [<sup>125</sup>I]IMPY to A $\beta$ (1–42) aggregates. As shown in Table 1, all the derivatives competed well with [<sup>125</sup>I]IMPY to bind the aggregates. The K<sub>i</sub> values estimated for **12**, **13**, **14**, **15**, and **16** were 14, 14, 15, 4, and 47 nM, respectively. The introduction into the DPOD backbone of an aminophenyl moiety, such as aminophenyl, methylaminophenyl or dimethylaminophenyl, resulted in good affinity. Further modification of the aminophenyl moiety with another electron-donating group, such as methoxyphenyl or hydroxyphenyl, resulted in a difference in binding to A $\beta$  aggregates, with the methoxy derivative **15** having 10-fold higher affinity than the hydroxy derivative **16**.

To confirm the affinity of DPOD derivatives for  $\beta$ -amyloid plaques in the AD brain, fluorescent staining of sections of mouse brain from an animal model of AD was carried out with compound **14** (Fig. 1). Many  $\beta$ -amyloid plaques were clearly stained with compound **14**, as reflected by the affinity for A $\beta$  aggregates in in vitro competition assays. The labeling pattern was consistent with that observed by immunohistochemical labeling with an antibody specific for A $\beta$ , indicating that DPOD derivatives show specific binding to  $\beta$ -amyloid plaques. Thus, the results suggest that DPOD



**Scheme 3.** (Bu<sub>3</sub>Sn)<sub>2</sub>, Pd(PhP<sub>3</sub>P), Et<sub>3</sub>N, dioxane; (b) I<sub>2</sub>, CHCl<sub>3</sub>; (c) [<sup>125</sup>I]NaI, H<sub>2</sub>O<sub>2</sub>, HCl.

**Table 1**

Inhibition constants for the binding of DPOD derivatives determined using [<sup>125</sup>I]IMPY as the ligand in Aβ(1–42) aggregates

Compound	K <sub>i</sub> <sup>a</sup> (nM)
<b>12</b>	14.2 ± 1.4
<b>13</b>	14.3 ± 3.6
<b>14</b>	15.4 ± 1.4
<b>15</b>	4.3 ± 2.1
<b>16</b>	47.1 ± 4.1

<sup>a</sup> Values are means ± standard error of the mean for 3–6 independent experiments.

derivatives may be applicable to the in vivo imaging of β-amyloid plaques in the brain.

To evaluate the uptake of DPOD derivatives in the brain, biodistribution experiments in normal mice were performed with four radioiodinated DPOD derivatives ([<sup>125</sup>I]**12**, [<sup>125</sup>I]**13**, [<sup>125</sup>I]**14**, and [<sup>125</sup>I]**15**), which showed strong affinity for Aβ aggregates in the in vitro-binding assays (Table 2). All four ligands penetrated the brain well with a delayed peak time at 30 and 60 min for uptakes (2.3–3.3%ID/g brain) in normal mice. But as a prerequisite for an imaging agent, they should be washed out from the normal brain, because there is no trapping mechanism for DPOD derivatives. Nevertheless, the long retention of these probes in the normal mouse brain suggested extensive non-specific binding which will contribute to a high level of background noise in vivo. Previously, we reported radioiodinated benzofuran derivatives as potential β-amyloid-binding agents.<sup>20</sup> The radioiodinated benzofurans penetrated the brain well with a peak uptake at 30–60 min postinjection, but a slow washout in normal mice prevents these probes from being used for imaging in vivo. More recently, we developed <sup>11</sup>C-labeled benzofuran derivatives, which are less lipophilic by replacing the iodine with a hydroxy group.<sup>21</sup> [<sup>11</sup>C]benzofuran showed a higher and faster peak of brain uptake and a faster washout from the brain in the normal mice. The improved properties in vivo observed with [<sup>11</sup>C]benzofuran make it a better candidate for the imaging of β-amyloid plaques. Indeed, the initial result obtained with [<sup>11</sup>C]benzofuran in a transgenic2576 mouse showed a relatively high S/N ratio.<sup>21</sup> Similar to [<sup>125</sup>I]benzofuran, the DPOD derivatives had unfavorable in vivo pharmacokinetics in normal mice, despite their good affinity for Aβ aggregates. Additional structural changes, that is, reducing the lipophilicity by introducing a hydrophilic group, are necessary to improve the in vivo properties of the DPOD derivatives.

### 3. Conclusion

In conclusion, we successfully designed and synthesized a new series of DPOD derivatives as probes for the in vivo imaging of β-amyloid plaques in the brain. The derivatives displayed excellent affinity for Aβ aggregates in in vitro-binding experiments. The de-

**Table 2**

Biodistribution of radioactivity after intravenous administration of [<sup>125</sup>I]**12**, [<sup>125</sup>I]**13**, [<sup>125</sup>I]**14**, and [<sup>125</sup>I]**15** in mice<sup>a</sup>

Tissue	Time after injection (min)			
	2	10	30	60
<b>[<sup>125</sup>I]12</b>				
Blood	4.55 (0.64)	2.32 (0.63)	3.09 (0.22)	2.99 (0.31)
Liver	21.36 (3.13)	17.37 (1.72)	14.89 (1.47)	12.33 (2.19)
Kidney	8.24 (1.26)	6.94 (0.70)	5.86 (0.56)	5.15 (0.74)
Intestine	1.50 (0.36)	3.08 (0.47)	5.84 (0.75)	8.33 (1.39)
Spleen	6.13 (1.67)	8.87 (2.35)	6.89 (0.81)	5.02 (0.55)
Pancreas	3.69 (2.30)	3.88 (0.54)	3.36 (0.36)	2.83 (0.32)
Heart	9.29 (1.66)	4.02 (0.48)	3.48 (0.24)	3.51 (0.61)
Stomach <sup>b</sup>	0.92 (0.31)	1.70 (0.18)	4.05 (0.96)	5.15 (1.32)
Brain	1.61 (0.23)	2.48 (0.16)	3.32 (0.31)	3.29 (0.58)
<b>[<sup>125</sup>I]13</b>				
Blood	3.54 (0.26)	1.84 (0.24)	1.52 (0.13)	1.54 (0.09)
Liver	14.62 (1.30)	12.37 (2.09)	8.53 (0.98)	7.30 (0.78)
Kidney	9.53 (0.83)	5.30 (0.94)	3.39 (0.66)	3.02 (0.58)
Intestine	1.36 (0.21)	2.83 (0.93)	5.67 (1.44)	8.46 (1.36)
Spleen	4.58 (0.62)	4.70 (0.48)	2.84 (0.35)	2.14 (0.22)
Pancreas	3.34 (0.38)	3.91 (0.60)	3.06 (0.58)	1.88 (0.25)
Heart	9.51 (0.77)	3.05 (0.50)	1.68 (0.21)	1.27 (0.20)
Stomach <sup>b</sup>	1.08 (0.11)	2.32 (0.62)	4.89 (0.99)	7.38 (0.97)
Brain	1.44 (0.12)	1.98 (0.36)	2.56 (0.44)	2.70 (0.33)
<b>[<sup>125</sup>I]14</b>				
Blood	5.42 (0.85)	2.41 (0.22)	1.79 (0.24)	1.56 (0.27)
Liver	13.94 (3.26)	8.27 (1.49)	5.89 (1.75)	5.15 (1.92)
Kidney	7.83 (3.53)	7.67 (1.62)	4.81 (1.01)	3.31 (0.77)
Intestine	1.59 (0.28)	2.40 (0.36)	4.12 (0.99)	5.37 (1.01)
Spleen	6.26 (1.53)	4.56 (1.11)	3.11 (0.62)	2.41 (0.29)
Pancreas	3.17 (0.73)	3.80 (0.50)	2.86 (1.64)	2.47 (0.62)
Heart	11.04 (2.43)	4.81 (1.07)	2.20 (0.54)	1.24 (0.68)
Stomach <sup>b</sup>	1.28 (0.21)	3.28 (0.36)	4.80 (0.56)	5.75 (2.47)
Brain	1.07 (0.23)	1.45 (0.27)	2.23 (0.61)	2.32 (0.64)
<b>[<sup>125</sup>I]15</b>				
Blood	1.96 (0.66)	1.63 (0.14)	1.23 (0.39)	1.12 (0.26)
Liver	11.94 (1.92)	9.35 (1.17)	6.13 (0.76)	4.44 (0.60)
Kidney	8.77 (1.17)	6.22 (0.87)	3.85 (1.01)	2.95 (0.66)
Intestine	1.70 (0.27)	3.53 (0.32)	6.62 (0.90)	8.21 (1.84)
Spleen	4.41 (0.72)	3.62 (0.28)	2.13 (0.53)	1.34 (0.40)
Pancreas	4.55 (0.77)	4.94 (0.26)	2.84 (0.48)	1.45 (0.28)
Heart	11.30 (1.92)	4.44 (0.67)	1.84 (0.32)	1.35 (0.29)
Stomach <sup>b</sup>	0.62 (0.21)	1.64 (0.10)	2.46 (0.80)	3.16 (1.39)
Brain	2.06 (0.45)	2.76 (0.23)	2.82 (0.34)	2.01 (0.33)

<sup>a</sup> Expressed as % injected dose per gram. Each value represents the mean (s.d.) for 3–5 animals at each interval.

<sup>b</sup> Expressed as % injected dose per organ.

gree to which the DPOD derivatives penetrated the brain was also very encouraging. However, non-specific binding in vivo reflected by a slow washout from the normal mouse brain makes them unsuitable for the imaging of β-amyloid plaques. The less than ideal in vivo biodistribution results in normal mice indicate that there is a critical need to fine-tune the kinetics of brain uptake and washout. Additional changes to the DPOD pharmacopore with

high-binding affinity for A $\beta$  aggregates may lead to useful probes for detecting  $\beta$ -amyloid plaques in the AD brain.

## 4. Experimental

### 4.1. General information

All reagents were commercial products and used without further purification unless otherwise indicated. <sup>1</sup>H NMR spectra were obtained on a Varian Gemini 300 spectrometer with TMS as an internal standard. Coupling constants are reported in Hertz. Multiplicity is defined by s (singlet), d (doublet), t (triplet), br (broad), and m (multiplet). Mass spectra were obtained on a JEOL IMS-DX instrument.

#### 4.1.1. 3-(4-Bromophenyl)-5-(4-nitrophenyl)-1,2,4-oxadiazole (1)

To a stirring solution of 4-bromobenzamidoxime (645 mg, 3 mmol) and 4-nitrobenzoic acid (495 mg, 3 mmol) in DMF (10 mL) was added a solution of DCC (3.6 mmol) and HOBT (6.0 mmol) in DMF (5 mL). The reaction mixture was stirred at room temperature for 18 h, and then at 100 °C for 2 h. The solvent was removed, and the residue was purified by silica gel chromatography (hexane/ethyl acetate = 9:1) to give 370 mg of **1** (35.6%). <sup>1</sup>H NMR (300 MHz, CDCl<sub>3</sub>)  $\delta$  7.70 (d, *J* = 8.7 Hz, 2H), 8.06 (d, *J* = 8.7 Hz, 2H), and 8.43 (s, 4H). MS *m/z* 346 (M<sup>+</sup>).

#### 4.1.2. 4-(3-(4-Bromophenyl)-1,2,4-oxadiazol-5-yl)aniline (2)

A mixture of **1** (350 mg, 1 mmol), SnCl<sub>2</sub> (948 mg, 5 mmol) and EtOH (15 mL) was stirred under reflux for 2 h. After the mixture had cooled to room temperature, 1 M NaOH (100 mL) was added until the mixture became alkaline. After extraction with ethyl acetate (100 mL  $\times$  2), the combined organic layer was washed with brine, dried over Na<sub>2</sub>SO<sub>4</sub>, and evaporated to give 258 mg of **2** (80.8%). <sup>1</sup>H NMR (300 MHz, CDCl<sub>3</sub>)  $\delta$  4.16 (s, 2H), 6.75 (d, *J* = 8.7 Hz, 2H), 7.63 (d, *J* = 8.4 Hz, 2H), 8.00 (d, *J* = 9.0 Hz, 2H), and 8.03 (d, *J* = 6.3 Hz, 2H). MS *m/z* 316 (M<sup>+</sup>).

#### 4.1.3. 4-(3-(4-Bromophenyl)-1,2,4-oxadiazol-5-yl)-*N*-methylaniline (3)

A solution of NaOCH<sub>3</sub> (28 wt% in MeOH, 0.4 mL) was added to a mixture of **2** (185 mg, 0.59 mmol) and paraformaldehyde (176 mg, 0.59 mmol) in methanol (10 mL) dropwise. The mixture was stirred under reflux for 30 min. After NaBH<sub>4</sub> (225 mg, 5.9 mmol) was added, the solution was heated under reflux for 1.5 h. 1 M NaOH (50 mL) was added to the cold mixture and extracted with CHCl<sub>3</sub> (50 mL). The organic phase was dried over Na<sub>2</sub>SO<sub>4</sub> and filtered. The solvent was removed, and the residue was purified by silica gel chromatography (hexane/ethyl acetate = 4:1) to give 98 mg of **3** (50.3%). <sup>1</sup>H NMR (300 MHz, CDCl<sub>3</sub>)  $\delta$  2.93 (s, 3H), 4.30 (s, 1H), 6.66 (d, *J* = 8.7 Hz, 2H), 7.63 (d, *J* = 8.7 Hz, 2H), 8.01 (d, *J* = 8.7 Hz, 2H), and 8.03 (d, *J* = 8.7 Hz, 2H). MS *m/z* 330 (M<sup>+</sup>).

#### 4.1.4. 4-(3-(4-Bromophenyl)-1,2,4-oxadiazol-5-yl)-*N,N*-dimethylaniline (4)

To a stirred mixture of **2** (35 mg, 0.10 mmol) and paraformaldehyde (36 mg, 1.2 mmol) in AcOH (5 mL) was added NaCNBH<sub>3</sub> (50 mg, 0.80 mmol) in one portion at room temperature. The resulting mixture was stirred at room temperature for 2 h. After 1 M NaOH (30 mL) was added and extraction with CH<sub>2</sub>Cl<sub>2</sub> (30 mL), the organic phase was dried over Na<sub>2</sub>SO<sub>4</sub>. The solvent was removed and the residue was purified by silica gel chromatography (hexane/ethyl acetate = 4:1) to give 24 mg of **4** (68.4%). <sup>1</sup>H NMR (300 MHz, CDCl<sub>3</sub>)  $\delta$  3.09 (s, 6H), 6.75 (d, *J* = 9.0 Hz, 2H), 7.63 (d, *J* = 8.4 Hz, 2H), 8.35 (d, *J* = 8.7 Hz, 2H), and 8.43 (d, *J* = 8.7 Hz, 2H). MS *m/z* 344.

#### 4.1.5. 3-(4-Bromophenyl)-5-(4-methoxyphenyl)-1,2,4-oxadiazole (5)

The same reaction as described above to prepare **1** was used, and 153 mg of **5** was obtained in a 23.1% yield from 4-bromobenzamidoxime and 4-anisic acid. <sup>1</sup>H NMR (300 MHz, CDCl<sub>3</sub>)  $\delta$  3.91 (s, 3H), 7.05 (d, *J* = 8.7 Hz, 2H), 7.65 (d, *J* = 8.7 Hz, 2H), 8.04 (d, *J* = 8.4 Hz, 2H), 8.15 (d, *J* = 9.0 Hz, 2H). MS *m/z* 330 (M<sup>+</sup>).

#### 4.1.6. 4-(3-(4-Bromophenyl)-1,2,4-oxadiazol-5-yl)phenol (6)

BBr<sub>3</sub> (4.5 mL, 1 M solution in CH<sub>2</sub>Cl<sub>2</sub>) was added to a solution of **5** (300 mg, 0.91 mmol) in CH<sub>2</sub>Cl<sub>2</sub> (10 mL) dropwise in an ice bath. The mixture was allowed to warm to room temperature and stirred for 42 h. Water (30 mL) was added while the reaction mixture was cooled in an ice bath. The mixture was extracted with chloroform (30 mL  $\times$  2) and the organic phase was dried over Na<sub>2</sub>SO<sub>4</sub> and filtered. The solvent was removed and the residue was purified by silica gel chromatography (hexane/ethyl acetate = 4:1) to give 146 mg of **6** (50.6%). <sup>1</sup>H NMR (300 MHz, CDCl<sub>3</sub>)  $\delta$  6.99 (d, *J* = 8.7 Hz, 2H), 7.65 (d, *J* = 8.7 Hz, 2H), 8.04 (d, *J* = 8.1 Hz, 2H), and 8.12 (d, *J* = 9.0 Hz, 2H). MS *m/z* 316 (M<sup>+</sup>).

#### 4.1.7. 4-(3-(4-(Tributylstannyl)phenyl)-1,2,4-oxadiazol-5-yl)aniline (7)

A mixture of **2** (100 mg, 0.32 mmol), bis(tributyltin) (0.2 mL) and (Ph<sub>3</sub>P)<sub>4</sub>Pd (16 mg, 0.014 mmol) in a mixed solvent (10 mL, 3:2 dioxane/triethylamine mixture) was stirred for 10 h under reflux. The solvent was removed, and the residue was purified by silica gel chromatography (hexane/ethyl acetate = 3:1) to give 28 mg of **7** (16.8%). <sup>1</sup>H NMR (300 MHz, CDCl<sub>3</sub>)  $\delta$  0.87–1.61 (m, 27H), 4.13 (s, 2H), 6.76 (d, *J* = 8.7 Hz, 2H), 7.59 (d, *J* = 8.1 Hz, 2H), 8.01 (d, *J* = 8.7 Hz, 1H), 8.07 (d, *J* = 8.1 Hz, 2H), and 8.28 (s, 1H).

#### 4.1.8. *N*-Methyl-4-(3-(4-(tributylstannyl)phenyl)-1,2,4-oxadiazol-5-yl)aniline (8)

The same reaction as described above to prepare **7** was employed, and 23 mg of **8** was obtained in a 15.8% yield from **3**. <sup>1</sup>H NMR (300 MHz, CDCl<sub>3</sub>)  $\delta$  0.87–1.63 (m, 27H), 2.92 (s, 3H), 4.27 (s, 1H), 6.66 (d, *J* = 8.7 Hz, 2H), 7.59 (d, *J* = 8.1 Hz, 2H), 8.03 (d, *J* = 8.4 Hz, 2H), and 8.08 (d, *J* = 7.8 Hz, 2H).

#### 4.1.9. *N,N*-Dimethyl-4-(3-(4-(tributylstannyl)phenyl)-1,2,4-oxadiazol-5-yl)aniline (9)

The same reaction as described above to prepare **7** was employed, and 45 mg of **9** was obtained in a 20.3% yield from **4**. <sup>1</sup>H NMR (300 MHz, CDCl<sub>3</sub>)  $\delta$  0.87–1.58 (m, 27H), 3.09 (s, 6H), 6.76 (d, *J* = 9.6 Hz, 2H), 7.59 (d, *J* = 8.1 Hz, 2H), 8.05 (d, *J* = 8.4 Hz, 2H), and 8.08 (d, *J* = 8.4 Hz, 2H).

#### 4.1.10. 5-(4-Methoxyphenyl)-3-(4-(tributylstannyl)phenyl)-1,2,4-oxadiazole (10)

The same reaction as described above to prepare **7** was employed, and 42 mg of **10** was obtained in a 22.8% yield from **5**. <sup>1</sup>H NMR (300 MHz, CDCl<sub>3</sub>)  $\delta$  0.87–1.59 (m, 27H), 3.91 (s, 3H), 7.04 (d, *J* = 8.7 Hz, 2H), 7.61 (d, *J* = 7.8 Hz, 2H), 8.07 (d, *J* = 9.0 Hz, 2H), and 8.17 (d, *J* = 9.0 Hz, 2H).

#### 4.1.11. 4-(3-(4-(Tributylstannyl)phenyl)-1,2,4-oxadiazol-5-yl)phenol (11)

The same reaction as described above to prepare **7** was employed, and 28 mg of **11** was obtained in a 60.1% yield from **6**. <sup>1</sup>H NMR (300 MHz, CDCl<sub>3</sub>)  $\delta$  0.87–1.58 (m, 27H), 6.99 (d, *J* = 9.0 Hz, 2H), 7.61 (d, *J* = 7.8 Hz, 2H), 8.07 (d, *J* = 8.7 Hz, 2H), and 8.12 (d, *J* = 8.7 Hz, 2H).

**4.1.12. 4-(3-(4-Iodophenyl)-1,2,4-oxadiazol-5-yl)aniline (12)**

To a solution of **7** (27 mg, 0.05 mmol) in  $\text{CHCl}_3$  (5 mL) was added a solution of iodine in  $\text{CHCl}_3$  (1 mL, 50 mg/mL) at room temperature. The mixture was stirred at room temperature for 10 min and a saturated  $\text{NaHSO}_3$  solution (25 mL) was added. The mixture was stirred for 5 min and the organic phase was separated. The aqueous phase was extracted with  $\text{CH}_2\text{Cl}_2$  (25 mL  $\times$  2), and the combined organic phase was dried over  $\text{Na}_2\text{SO}_4$  and filtered. The solvent was removed and the residue was washed with hexane to give 12 mg of **12** (66.1%).  $^1\text{H NMR}$  (300 MHz,  $\text{CDCl}_3$ )  $\delta$  4.15 (s, 2H), 6.76 (d,  $J = 8.7$  Hz, 2H), 7.83 (d,  $J = 8.4$  Hz, 2H), 7.89 (d,  $J = 8.4$  Hz, 2H), and 8.01 (d,  $J = 8.7$  Hz, 2H). HRMS  $m/z$   $\text{C}_{14}\text{H}_{10}\text{N}_3\text{OI}$  found 362.9855/ calcd 362.9869 ( $\text{M}^+$ ).

**4.1.13. 4-(3-(4-Iodophenyl)-1,2,4-oxadiazol-5-yl)-*N*-methylaniline (13)**

The same reaction as described above to prepare **12** was employed and 20 mg of **13** was obtained in a 86.0% yield from **8**.  $^1\text{H NMR}$  (300 MHz,  $\text{CDCl}_3$ )  $\delta$  2.93 (s, 3H), 4.29 (s, 1H), 6.66 (d,  $J = 8.4$  Hz, 2H), 7.85 (d,  $J = 8.4$  Hz, 2H), 7.88 (d,  $J = 8.4$  Hz, 2H), and 8.02 (d,  $J = 8.4$  Hz, 2H). HRMS  $m/z$   $\text{C}_{15}\text{H}_{12}\text{N}_3\text{OI}$  found 377.0022/ calcd 377.0025 ( $\text{M}^+$ ).

**4.1.14. 4-(3-(4-Iodophenyl)-1,2,4-oxadiazol-5-yl)-*N,N*-dimethylaniline (14)**

The same reaction as described above to prepare **12** was employed and 34 mg of **14** was obtained in a 72.4% yield from **9**.  $^1\text{H NMR}$  (300 MHz,  $\text{CDCl}_3$ )  $\delta$  3.09 (s, 6H), 6.75 (d,  $J = 9.3$  Hz, 2H), 7.83 (d,  $J = 8.7$  Hz, 2H), 7.90 (d,  $J = 8.7$  Hz, 2H), and 8.04 (d,  $J = 9.3$  Hz, 2H). HRMS  $m/z$   $\text{C}_{16}\text{H}_{14}\text{N}_3\text{OI}$  found 391.0192/ calcd 391.0182 ( $\text{M}^+$ ).

**4.1.15. 3-(4-Iodophenyl)-5-(4-methoxyphenyl)-1,2,4-oxadiazole (15)**

The same reaction as described above to prepare **12** was employed and 17 mg of **15** was obtained in a 69.2% yield from **10**.  $^1\text{H NMR}$  (300 MHz,  $\text{CDCl}_3$ )  $\delta$  3.89 (s, 3H), 6.97 (d,  $J = 9.3$  Hz, 2H), 7.48 (d,  $J = 8.4$  Hz, 2H), 7.80 (d,  $J = 9.3$  Hz, 2H), and 7.85 (d,  $J = 9.0$  Hz, 2H). HRMS  $m/z$   $\text{C}_{15}\text{H}_{11}\text{N}_2\text{O}_2\text{I}$  found 377.9865/ calcd 377.9872 ( $\text{M}^+$ ).

**4.1.16. 4-(3-(4-Iodophenyl)-1,2,4-oxadiazol-5-yl)phenol (16)**

The same reaction as described above to prepare **12** was employed and 14 mg of **16** was obtained in a 81.8% yield from **11**.  $^1\text{H NMR}$  (300 MHz,  $\text{CDCl}_3$ )  $\delta$  6.99 (d,  $J = 8.7$  Hz, 2H), 7.87 (d,  $J = 8.4$  Hz, 2H), 7.88 (d,  $J = 8.1$  Hz, 2H), and 8.12 (d,  $J = 8.1$  Hz, 2H). HRMS  $m/z$   $\text{C}_{14}\text{H}_9\text{N}_2\text{O}_2\text{I}$  found 363.9704/ calcd 363.9709 ( $\text{M}^+$ ).

**4.2. Iododestannylation reaction**

The radioiodinated forms of compounds **12**, **13**, **14**, and **15** were prepared from the corresponding tributyltin derivatives by iododestannylation. Briefly, to initiate the reaction, 50  $\mu\text{L}$  of  $\text{H}_2\text{O}_2$  (3%) was added to a mixture of a tributyltin derivative (100  $\mu\text{g}/50$   $\mu\text{L}$  EtOH), [ $^{125}\text{I}$ ]NaI (0.1–0.2 mCi, specific activity 2200 Ci/mmol), and 100  $\mu\text{L}$  of 1 N HCl in a sealed vial. The reaction was allowed to proceed at room temperature for 10 min and terminated by addition of  $\text{NaHSO}_3$ . After neutralization with sodium bicarbonate and extraction with ethyl acetate, the extract was dried by passing it through an anhydrous  $\text{Na}_2\text{SO}_4$  column and then blown dry with a stream of nitrogen gas. The radioiodinated ligand was purified by HPLC on a Cosmosil C18 column with an isocratic solvent of  $\text{H}_2\text{O}/\text{acetonitrile}$  (3/7) at a flow rate of 1.0 mL/min. The purified ligand was stored at  $-20$   $^\circ\text{C}$  for the in vitro binding and biodistribution experiments.

**4.3. Binding assays using the aggregated A $\beta$  peptide in solution**

A solid form of A $\beta$ (1–42) was purchased from Peptide Institute (Osaka, Japan). Aggregation of peptides was carried out by gently dissolving the peptide (0.25 mg/mL) in a buffer solution (pH 7.4) containing 10 mM sodium phosphate and 1 mM EDTA. The solutions were incubated at 37  $^\circ\text{C}$  for 42 h with gentle and constant shaking. Binding experiments were carried out as described previously.<sup>22</sup> [ $^{125}\text{I}$ ]IMPY (6-iodo-2-(4'-dimethylamino)phenyl-imidazo[1,2]pyridine) with 2200 Ci/mmol specific activity and greater than 95% radiochemical purity was prepared using the standard iododestannylation reaction as described previously.<sup>13</sup> Binding assays were carried out in 12  $\times$  75 mm borosilicate glass tubes. The reaction mixture contained 50  $\mu\text{L}$  of A $\beta$ (1–42) aggregates (29 nM in the final assay mixture), 50  $\mu\text{L}$  of [ $^{125}\text{I}$ ]IMPY (0.02 nM diluted in 10% EtOH), 50  $\mu\text{L}$  of inhibitor (8 pM–12.5  $\mu\text{M}$  diluted in 10% EtOH), and 850  $\mu\text{L}$  of 10% EtOH. Non-specific binding was defined in the presence of 400 nM IMPY in the same assay tubes. The mixture was incubated at 37  $^\circ\text{C}$  for 3 h and the bound and the free radioactivities were separated by vacuum filtration through Whatman GF/B filters using a Brandel M-24R cell harvester followed by 2  $\times$  3 mL washes with 10% EtOH at room temperature. Filters containing the bound I-125 ligand were placed in a gamma counter (Aloka, ARC-380) for measuring radioactivity. Under the assay conditions, the specifically bound fraction accounted for less than 15% of the total radioactivity. Values for the half-maximal inhibitory concentration ( $\text{IC}_{50}$ ) were determined from displacement curves using GraphPad Prism 4.0 (GraphPad Software, San Diego, CA), and those for the inhibition constant ( $K_i$ ) were calculated using the Cheng-Prusoff equation.<sup>23</sup>

**4.4. Neuropathological staining of model mouse brain sections**

The Tg2576 transgenic mice (female, 23-month-old) were used as Alzheimer's model mice. After the mice were sacrificed by decapitation, the brains were immediately removed and frozen in powdered dry ice. The frozen blocks were sliced into serial sections, 10- $\mu\text{m}$  thick. Each slide was incubated with a 50% ethanol solution (100  $\mu\text{M}$ ) of compound **14**. The sections were washed in 50% ethanol for 3 min two times. Fluorescent observation was performed with the Nikon system. Thereafter, the serial sections were also immunostained with DAB as a chromogen using monoclonal antibodies against  $\beta$ -amyloid (Amyloid  $\beta$ -Protein Immunohistochemistry kit, WAKO).

**4.5. In vivo biodistribution in normal mice**

The experiments with animals were conducted in accordance with our institutional guidelines and were approved by Nagasaki University Animal Care Committee. A saline solution (100  $\mu\text{L}$ ) containing ethanol (10  $\mu\text{L}$ ) of radiolabeled agents (0.5  $\mu\text{Ci}$ ) was injected intravenously directly into the tail vein of ddY mice (5-week-old, 22–25 g). The mice were sacrificed at various time points post-injection. The organs of interest were removed and weighed, and the radioactivity was measured with an automatic gamma counter (Aloka, ARC-380).

**Acknowledgments**

This study was supported by the Program for Promotion of Fundamental Studies in Health Sciences of the National Institute of Biomedical Innovation (NIBIO) and Health Labour Sciences Research Grant.

**References and notes**

- Selkoe, D. J. *Physiol. Rev.* **2001**, *81*, 741.
- Hardy, J.; Selkoe, D. J. *Science* **2002**, *297*, 353.

3. Selkoe, D. J. *Nat. Biotechnol.* **2000**, *18*, 823.
4. Nordberg, A. *Lancet Neurol.* **2004**, *3*, 519.
5. Mathis, C. A.; Wang, Y.; Klunk, W. E. *Curr. Pharm. Des.* **2004**, *10*, 1469.
6. Agdeppa, E. D.; Kepe, V.; Liu, J.; Flores-Torres, S.; Satyamurthy, N.; Petric, A.; Cole, G. M.; Small, G. W.; Huang, S. C.; Barrio, J. R. *J. Neurosci.* **2001**, *21*, RC189.
7. Shoghi-Jadid, K.; Small, G. W.; Agdeppa, E. D.; Kepe, V.; Ercoli, L. M.; Siddarth, P.; Read, S.; Satyamurthy, N.; Petric, A.; Huang, S. C.; Barrio, J. R. *Am. J. Geriatr. Psychiatry* **2002**, *10*, 24.
8. Mathis, C. A.; Wang, Y.; Holt, D. P.; Huang, G. F.; Debnath, M. L.; Klunk, W. E. *J. Med. Chem.* **2003**, *46*, 2740.
9. Klunk, W. E.; Engler, H.; Nordberg, A.; Wang, Y.; Blomqvist, G.; Holt, D. P.; Bergstrom, M.; Savitcheva, I.; Huang, G. F.; Estrada, S.; Ausen, B.; Debnath, M. L.; Barletta, J.; Price, J. C.; Sandell, J.; Lopresti, B. J.; Wall, A.; Koivisto, P.; Antoni, G.; Mathis, C. A.; Langstrom, B. *Ann. Neurol.* **2004**, *55*, 306.
10. Ono, M.; Wilson, A.; Nobrega, J.; Westaway, D.; Verhoeff, P.; Zhuang, Z. P.; Kung, M. P.; Kung, H. F. *Nucl. Med. Biol.* **2003**, *30*, 565.
11. Verhoeff, N. P.; Wilson, A. A.; Takeshita, S.; Trop, L.; Hussey, D.; Singh, K.; Kung, H. F.; Kung, M. P.; Houle, S. *Am. J. Geriatr. Psychiatry* **2004**, *12*, 584.
12. Rowe, C. C.; Ackerman, U.; Browne, W.; Mulligan, R.; Pike, K. L.; O'Keefe, G.; Tochon-Danguy, H.; Chan, G.; Berlangieri, S. U.; Jones, G.; Dickinson-Rowe, K. L.; Kung, H. P.; Zhang, W.; Kung, M. P.; Skovronsky, D.; Dyrks, T.; Holl, G.; Krause, S.; Friebe, M.; Lehman, L.; Lindemann, S.; Dinkelborg, L. M.; Masters, C. L.; Villemagne, V. L. *Lancet Neurol.* **2008**, *7*, 129.
13. Kung, M.; Kung, M. P.; Hou, C.; Zhuang, Z. P.; Zhang, B.; Skovronsky, D.; Trojanowski, J. Q.; Lee, V. M.; Kung, H. F. *Brain Res.* **2002**, 956, 202.
14. Newberg, A. B.; Wintering, N. A.; Plossl, K.; Hochold, J.; Stabin, M. G.; Watson, M.; Skovronsky, D.; Clark, C. M.; Kung, M. P.; Kung, H. F. *J. Nucl. Med.* **2006**, *47*, 78.
15. Qu, W.; Kung, M. P.; Hou, C.; Oya, S.; Kung, H. F. *J. Med. Chem.* **2007**, *50*, 3380.
16. Chandra, R.; Kung, M. P.; Kung, H. F. *Bioorg. Med. Chem. Lett.* **2006**, *16*, 1350.
17. Santagada, V.; Frecentese, F.; Perissutti, E.; Cirillo, D.; Terracciano, S.; Caliendo, G. *Bioorg. Med. Chem. Lett.* **2004**, *14*, 4491.
18. Barluenga, A. M.; Bayron, G.; Asensio, A. *J. Chem. Soc., Chem. Commun.* **1984**, 1334.
19. Gribble, G. W.; Nutaitis, C. F. *Synthesis* **1987**, 709.
20. Ono, M.; Kung, M. P.; Hou, C.; Kung, H. F. *Nucl. Med. Biol.* **2002**, *29*, 633.
21. Ono, M.; Kawashima, H.; Nonaka, A.; Kawai, T.; Haratake, M.; Mori, H.; Kung, M.-P.; Kung, H. F.; Saji, H.; Nakayama, M. *J. Med. Chem.* **2006**, *49*, 2725.
22. Kung, M. P.; Hou, C.; Zhuang, Z. P.; Skovronsky, D.; Kung, H. F. *Brain Res.* **2004**, *1025*, 98.
23. Cheng, Y.; Prusoff, W. H. *Biochem. Pharmacol.* **1973**, *22*, 3099.